Translational Oncology
www.transonc.com

Volume 4 Number 2 April 2011 pp. 101–109 **101**

Role of SOCS-1 Gene on Melanoma Cell Growth and Tumor Development[1]

Jorge A. Borin Scutti*, Alisson Leonardo Matsuo*, Felipe Valença Pereira*, Mariana Hiromi Massaoka*, Carlos Rogério Figueiredo*, Dayson Friaça Moreira†, José Ernesto Belizário† and Luiz R. Travassos*

*Experimental Oncology Unit, Department of Microbiology, Immunology and Parasitology, Federal University of São Paulo, São Paulo, SP, Brazil; †Department of Pharmacology, University of São Paulo, São Paulo, SP, Brazil

Abstract

Melanoma is the most aggressive form of skin cancer, and its incidence has increased dramatically over the years. The murine B16F10 melanoma in syngeneic C57Bl/6 mice has been used as a highly aggressive model to investigate tumor development. Presently, we demonstrate in the B16F10-Nex2 subclone that silencing of SOCS-1, a negative regulator of Jak/Stat pathway, leads to reversal of the tumorigenic phenotype and inhibition of melanoma cell metastasis. SOCS-1 silencing with short hairpin RNA affected tumor growth and cell cycle regulation with arrest at the S phase with large-sized nuclei, reduced cell motility, and decreased melanoma cell invasion through Matrigel. A clonogenic assay showed that SOCS-1 acted as a modulator of resistance to anoikis. In addition, down-regulation of SOCS-1 decreased the expression of epidermal growth factor receptor (mainly the phosphorylated-R), Ins-Rα, and fibroblast growth factor receptor. *In vivo*, silencing of SOCS-1 inhibited subcutaneous tumor growth and metastatic development in the lungs. Because SOCS-1 is expressed in most melanoma cell lines and bears a relation with tumor invasion, thickness, and stage of disease, the present results on the effects of SOCS-1 silencing in melanoma suggest that this regulating protein can be a target of cancer therapy.

Translational Oncology (2011) 4, 101–109

Introduction

Malignant melanoma is the most invasive and deadly skin cancer with increasing incidence [1,2]. Tumor cell induction, invasion, and metastasis have been intensely studied, and numerous receptors, mediators, and signaling pathways have been identified [3,4]. The understanding of the regulatory pathways involved in melanoma development and progression has advanced significantly in recent years [5]. Among these pathways, those involving Ras, B-Raf, MEK, PTEN, phosphatidylinositol-3 kinase, and Akt are constitutively activated in melanoma [6]. The Ras-Raf-MEK 1, 2–ERK 1, 2 cascade is activated by growth factors and has been implicated in cell proliferation, differentiation, and survival [7]. Another signaling pathway activated by growth factor receptors involves the phosphorylation of signal transducers and activators of transcription (STAT).

The JAK/STAT pathways have been implicated in tumor promotion, migration, and invasive growth [8–12]. Pleiotropic STATs in these pathways are negatively regulated by suppressor of cytokine signaling (SOCS) proteins [13–15]. There are eight members in the SOCS family (CIS and SOCS 1-7). Each one has a central SH2 domain, an amino-terminal domain of variable length and sequence, and a 40–amino acid module on the carboxy-terminal region that is known as the SOCS box [16]. The SOCS box mediates interaction with elongin B and C, cullin-5, and RING-box-2 (RBX2), which recruits E2 ubiquitin transferase [17]. The SOCS family of proteins as well as other SOCS-box–containing molecules, probably functions as E3 ubiquitin ligases and facilitates the degradation of proteins that are associated with members of this family through their N-terminal regions. The *SOCS-1* expression product, focused on in the present work, interacts with the microtubule organizing complex and may target JAKs [18].

Address all correspondence to: Luiz R. Travassos, MD, PhD, Unidade de Oncologia Experimental (UNONEX), Departamento de Microbiologia, Imunologia e Parasitologia, UNIFESP, Rua Botucatu, 862, oitavo andar, São Paulo, SP 04023-062, Brazil.
E-mail: travassos@unifesp.br

[1]The present work was supported by the Fundação de Amparo a Pesquisa do Estado de São Paulo grant 06/50634-2 and CNPq.
Received 13 October 2010; Revised 6 December 2010; Accepted 9 December 2010

DOI 10.1593/tlo.10250

SOCS-1 suppresses the cellular response to various cytokines including interleukin-6 (IL-6), IL-4, leukemia inhibitor factor, oncostatin M, interferon (IFN), and growth hormones. The main regulatory function of SOCS-1 is to inhibit cytokine signal transduction through direct interaction with active JAK-2 by binding to their activation loop through its SH2 domain [19]. In fact, many studies have demonstrated the role of SOCS protein on cytokine signaling, including the immune suppression and cytokine resistance [20–22]. In relation to tumor cells, studies have focused on the tumor response to cytokines as a function of SOCS protein expression. Zitzmann et al. [22] showed that silencing of SOCS-1 expression by small interfering RNA (siRNA) enhanced the antitumor effects of type I IFNs on neuroendocrine tumor cells. Down-regulation of basal Bcl-2 and Bcl-xL and up-regulation of basal Bak and Bax accompanied silencing of SOCS-1. The antiproliferative effect of IFN-β and IFN-γ was also shown in tumor cells on silencing of SOCS-1 [23]. In human melanoma, siRNA inhibition of SOCS-1 and SOCS-3 expression enhanced their responsiveness to IFN-α and IFN-γ stimulation [24], and the progression of melanoma cells from IFN-γ sensitivity to IFN-γ resistance was associated with attenuation of SOCS genes induction and constitutive expression of SOCS-3 [25]. Li et al. [26] showed that normal and transformed human melanocyte cells constitutively express SOCS-1 transcripts *in vitro*, whereas the SOCS-1 protein was found only in melanoma cells. In contrast, Yoshikawa et al. [21] showed that SOCS-1 protein acted as a tumor suppressor gene in hepatocellular carcinoma cells. Thus, the role of SOCS-1 in tumor development and progression seems to be cell type–specific, with *SOCS-1* acting either as a tumor suppressor gene or as a marker of progression in melanoma [27,28].

In the present study, we examined the short hairpin RNAi (shRNAi) silencing of *SOCS-1* in B16F10-Nex2 melanoma cells to address the mechanisms governing development and progression of melanoma and to evaluate the SOCS-1 protein as a promising target for cancer therapy.

Materials and Methods

Cell Lines and Stable Transduction

B16F10 murine melanoma cells were originally obtained from the Ludwig Institute for Cancer Research in São Paulo. Different sublines (Nex) were isolated at the Experimental Oncology Unit (UNONEX) with different characteristics including the serum source used for *in vitro* subculturing [29]. The subline B16F10-Nex2 with medium invasiveness capacity *in vivo* was presently used. Cell lines were the B16F10-Nex2 clone (B16), the cell line transduced with the empty (control) lentivirus vector (B16 LVc), and the cell line transduced with the shRNAi SOCS-1 construction (B16 shR-SOCS-1). They were cultured in RPMI-1640 supplemented with 10 mM HEPES, 24 mM sodium bicarbonate, 40 mg/ml gentamicin, and 10% fetal calf serum (FCS), pH 7.4, at 37°C and 5% CO_2.

Plasmid, Transduction, and Transfection

For stable silencing of the *SOCS-1* gene, we generated lineages with the specific construction. Plasmid pLKO.1 (Addgene, Cambridge, MA) and the annealed insert corresponding to the shRNAi for *SOCS-1* gene were cleaved at cloning sites with restriction enzymes *Age*I and *Eco*RI (Invitrogen, San Diego, CA). The insert was then ligated into the plasmid and transformed into *Escherichia coli* strain DH5α with ampicillin resistance gene. The sequences of SOCS-1 sense and antisense oligonucleotides used were described by Takahashi et al. [23], with modifications and synthesized by PeproTech (Rocky Hill, NJ).

Sense
5′CCGGCTACCTGAGTTCCTTCCCCTTCTCGAGAAGGGGAAGGAACTCAGGTAGTTTTTG 3′
Antisense
5′AATTCAAAAACTACCTGAGTTCCTTCCCCTTCTCGAGAAGGGGAAGGAACTCAGGTAG 3′

To expand the plasmid, DH5α bacteria were transformed by heat shock with the vectors, which were purified by mini-prep or maxi-prep alkaline. The plasmid was then sequenced at the Center for Human Genome Studies (São Paulo, Brazil), 350 ng/ml by sample using MegaBACE 1000 (GE Healthcare, Piscataway, NJ). The sequencing reactions were performed according to the MegaBACE 1000 protocol using the DYEnamic ET Dye Terminator Kit (with Thermo Sequenase II DNA polymerase; GE Healthcare) code US81090. The sequences were analyzed with the Sequence Analyser software (GE Healthcare) using the Base Caller Cimarron 3.12 (GE Healthcare). The recombinant lentivirus was produced by transfecting HEK 293 cells with the pLKO vector, MD2G packaging plasmid, and PAX2 envelope plasmid (Addgene) as described below. The B16F10-Nex2 cells were seeded in six-well plates (5×10^5 cell/well) and, 16 hours later, transduced with the virus at a multiplicity of infection of 5. After cell transduction with the control pLKO virus, the population of puromycin-resistant cells was selected.

Construction of the Lentiviral Particle shRNAi SOCS-1

The synthesis of viral particles was performed following the manufacturer's instruction (Addgene). The first step was to transfect HEK-293 cells (human kidney) with a mixture of plasmids, each imprinting a particular structural feature in the viral particle. Thus, 1 mg of total pLKO containing the specific construction SOCS-1, 750 ng of psPAX (packing), 250 ng of pMD2G (viral envelope), and 7×10^5 HEK-293 cells were plated on 12-well plates with Dulbecco modified Eagle medium (Invitrogen) supplemented with 20% FCS, at a confluence of 60% to 80% at 37°C and 5% CO_2. After 16 hours, the supernatant was removed, and the viral particles were stored at −80°C.

Flow Cytometry Analysis of Growth Factor Receptors

The tumor cells (10^6 cells in suspension) were fixed and treated with PBS containing 1% paraformaldehyde, 0.5% saponin, 1% BSA, and 1% mouse serum for 20 minutes at 4°C. Cells were washed in buffer A (PBS containing 0.5% saponin, 1% BSA, and 1% mouse serum) and incubated in the same buffer with antibodies to Insulin-Rα, Insulin-Rβ, epidermal growth factor receptor (EGFR), p-EGFR, and fibroblast growth factor receptors 3, 4, and 5 (FGFR-3, -4, and -5; Santa Cruz Biotechnology, Santa Cruz, CA) for 1 hour at 4°C, washed again, and incubated with anti–rabbit Ig conjugated with a fluorochrome (phycoerythrin) for 1 hour at 4°C. Cells were washed twice with buffer A and fixed with 0.4% paraformaldehyde. Fluorescence was measured on a FACScan flow cytometer (BD Biosciences, Franklin Lakes, NJ), and data were analyzed by FlowJo software (TriStar, Ashland, OR).

Cell Cycle Phases

The tumor cells (10^6 cells in suspension) were fixed and treated with PBS containing 2% of paraformaldehyde for 15 minutes at 4°C on a rotating table. Cells were washed three times with PBS and resuspended in 1 ml of 70% ethanol in PBS for 1 hour on ice. After further

washing in PBS, cells were resuspended in 1 ml of DNA staining solution (2.5 μg/ml propidium iodide and 0.5 mg/ml RNase A in PBS) and examined on a FACScan flow cytometer (BD Biosciences). Data were analyzed by CellQuest software (Becton Dickinson, San Jose, CA).

Fluorescence Microscopy with 4′,6-Diamidino-2-phenylindole and Phalloidin

To evaluate the morphology of the cell lines, 2×10^4 cells were seeded on sterilized round coverslips (Fisher Scientific Co, Pittsburgh, PA) inserted into 24-well plates and allowed to reach 80% confluence. After incubation, the coverslips were washed with PBS 1×, and cells were fixed with 2% of cold paraformaldehyde for 30 minutes. The cells were washed again and permeabilized with 0.1% Triton X-100 in PBS for 40 minutes. Cells were washed again and incubated with phalloidin-tetramethyl rhodamine isothiocyanate (1:1000; Invitrogen) and 1 mg/ml of 4′,6-diamidino-2-phenylindole (DAPI) diluted in PBS for 1 hour. Coverslips were anchored onto slides in the presence of 4 μl of Vectashield (Sigma), and nuclear and cytoplasm sizes and morphology were observed in a fluorescence microscope at 60× magnification in oil. DAPI staining (blue) was observed at 350 nm excitation and 470 nm emission, and fluorescein isothiocyanate (red) was observed at 490 and 520 nm, respectively. To phalloidin-TRITC (red actin), a filter was used, at 580 nm excitation and 604 nm emission. The nuclear areas of cells were calculated as in ellipsoids, as $\pi D/2d/2$, taking D (long) and d (short) as diameters.

Monolayer Wound Healing Assay

The tumor cells (B16, B16 LVc, and B16 shR-SOCS-1), 5×10^5, were seeded in six-well plates and allowed to reach complete confluence. To make the wound, the growth medium was aspirated and replaced by calcium-free PBS. A blue plastic P1000 pipette tip was used to scratch the cell monolayer off, to create a clear area. Fresh medium was added, and the wounds were observed using a phase-contrast microscope. Images were taken at regular intervals up to 24 hours and were analyzed by digitally drawing lines (using Adobe Photoshop) and averaging the positions of the migrating cells at the edges.

Invasion Assay through Matrigel

The invasion assay was performed using BioCoat Matrigel invasion chambers (BD Biosciences) primed according to the manufacturer's directions. A total of 5×10^3 tumor cells were used in this experiment. A solution of 20% FBS in RPMI 1640 or RPMI 1640 was placed in the lower well to act as a chemoattractant. Serum-free medium was added on the upper chamber of the Matrigel plate, and cells were incubated at 37°C for 24 hours. Invading cells detected on the bottom of the filter were stained with Protocol Hema3 stain set (Fisher Scientific). Cells unable (upper surface of filter) to invade the membrane were removed with a swab. Samples were analyzed in a Nikon Microphot-FXA microscope (Nikon, Inc, Melville, NY) at 10×, pictures were taken using Leica DFC 320 R2 (Leica Microsystems, Richmond, IL), and images were evaluated by Photoshop. Data are expressed as the average number of cells from four fields on the lower filter membrane surface.

Clonogenic Assay

The tumor cells (5×10^3) from each line were plated on 1% agarose medium, and diluted in RPMI 1640 plus 20% FCS. Thirty days after plating, the ability of the different cell lines to form colonies reflected resistance to anoikis and potential malignance. Colonies were counted with an optical microscope.

Western Blot Analysis

Cell lysates were prepared by sonication, and the SOCS-1 and actin were detected in 30 μg of total protein by 10% SDS-PAGE and transferred to a membrane (Millipore, Billerica, MA) for immunoblot analysis. The membranes were washed in Tris-buffered saline with Tween 20 (10 mM Tris-HCl, pH 8, 150 mM NaCl, and 0.05% Tween 20) and blocked with 5% skim milk in Tris-buffered saline with Tween 20 overnight at 4°C with shaking. The blots were then probed overnight at 4°C with primary antibodies for detection of murine α-SOCS-1 at 3 μg/ml (Invitrogen). After 2 hours of incubation with 1:1000 mouse peroxidase–conjugated secondary antibody (Invitrogen), the immunoreactive proteins were detected by enhanced chemiluminescence using the ECL detection system (GE Healthcare).

Messenger RNA Quantification

Total RNA was isolated using TRIzol (Invitrogen). To eliminate DNA contamination, total RNA was treated with DNase I (Sigma-Aldrich) before reverse transcription (RT). RT was performed using a SuperScript II (Gibco BRL, San Diego, CA) and dT-primer following the manufacturer's protocol. For quantitative mRNA expression analysis, real-time polymerase chain reaction (PCR) was carried out with total complementary DNA using ABI Prism 7700 Sequence Detector (Applied Biosystems, San Diego, CA). The sequences of the primers (SOCS-1 and HPRT) used for amplification were as follows:

5′ CCCTCGAGTAGGATGGTAGC 3′ and
5′ ACGAAGACGAGGACGAGGAG 3′;
5′-AAGGACCTCTCGAAGTGTTGGATA 3′ and
5′-CATTTAAAAGGAACTGTTGACAACG 3′.

Amplified products were detected online through intercalation of the fluorescent dye SYBR green (LightCycler-FastStart DNA Master SYBR Green I Kit; Roche Diagnostics, Indianapolis, IN). The conditions used were as follows: initial enzyme activation at 95°C for 10 minutes, followed by 55 cycles at 95°C for 10 seconds, 60°C for 5 seconds, and 72°C for 15 seconds. Gene-specific fluorescence was measured at 72°C. The mRNA expression of target genes was normalized by using the mRNA level of HPRT.

Cell Proliferation

The tumor cells (5×10^4) of each cell line were seeded in Petri dishes for measuring the growth kinetics after 0, 24, 48, 72, 96, and 120 hours. The cells were collected in PBS–0.02% EDTA resuspended in serum-free RPMI, and 20 μl of this suspension was used for cell counting in a Neubauer chamber. The counting was performed in triplicate using Trypan blue exclusion for viable cells.

Animals and Tumor Development In Vivo

Male C57Bl/6 mice (CEDEME, UNIFESP), 6 to 8 weeks old, were housed under specific pathogen-free conditions. When subcutaneously challenged with B16F10-Nex2 melanoma cells, animals were killed when tumors reached a maximum of 3000 mm^3. Subcutaneous challenges were made with 5×10^4 tumor cells of each cell line (95% viability by Trypan blue exclusion test) in 0.2 ml of buffered saline into the right flank of each mouse ($n = 6$ per group). Tumor growth was recorded with a caliper and calculated as $V = 0.52 \times d^2 \times D$

(*D*, long diameter; *d*, short diameter). In the metastatic model, 5×10^5 tumor cells of each cell line were injected into the tail veins of mice (0.1 ml per mouse). Fifteen days later, mice ($n = 5$ per group) were killed, their lungs were harvested, and the number of macroscopic tumor nodules were counted. All experiments with animals were approved by the ethical committee of the Federal University of São Paulo.

Statistical Analyses

Data presented as means ± SEs were compared by two-sided Student's *t* test or by analysis of variance, and when appropriate, we used the Instat software version 3.05 (GraphPad, San Diego, CA). Real-time PCR was analyzed by REST 2008, and data were considered statistically significant when $P < .05$.

Results

SOCS-1 Expression in B16F10-Nex2 Melanoma Cells

RT-PCR and Western blot analyses showed that the cell lines B16 LVc and B16 expressed SOCS-1 constitutively, whereas SOCS-1 expression in B16 shR-SOCS-1 was much reduced. The relative expression of SOCS-1 in these cell lines compared with the total expression in B16 (B16F10-Nex2 cells) is shown in Figure 1*A*. The expression of SOCS-1 protein (25 kDa) was silenced in the shRNAi-transduced cells (Figure 1*B*). Silencing of 83% relative to the control was normalized using the housekeeping gene *HPRT* and the method $2^{-\Delta\Delta Ct}$, with software REST 2008 based on their Web site: http://www.gene-quantification.de/pfaffl-et-al-nar-2002.pdf.

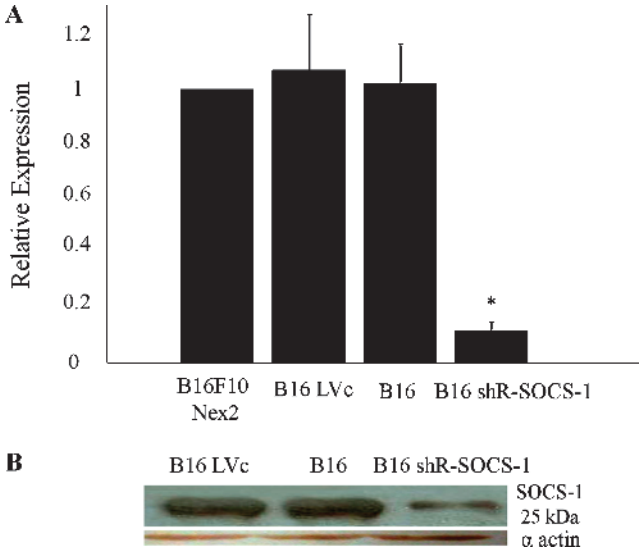

Figure 1. The effectiveness of shRNAi silencing of SOCS-1 protein. (A) RT-PCR showing 83% reduction in SOCS-1 expression in B16 shR-SOCS-1 transduced cells compared with the original B16F10-Nex2 cell line, a derived clone (B16), and the cell line transduced with the empty (control) lentivirus vector (B16 LVc). (B) Western blot analysis showing the reduced expression of SOCS-1 in B16F10-Nex2 cell line stably transduced with shRNAi compared with control cell lines. α-Actin was used as the constitutive expression control.

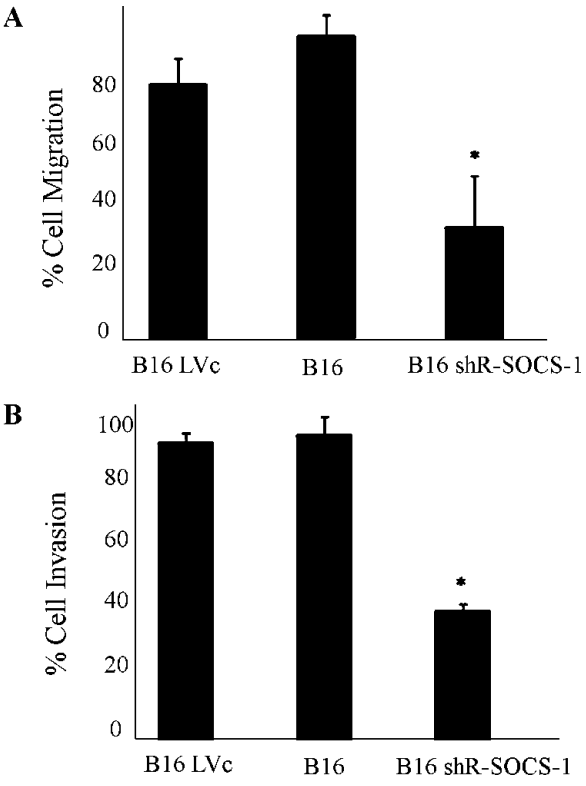

Figure 2. The silencing of SOCS-1 decreases cell motility and invasion of melanoma cells. (A) By using the wound healing assay on monolayers of 5×10^5 cells, the percent migrations of B16, B16 LVc, and B16 shR-SOCS-1 were 63%, 75%, and 28% respectively. (B) The invasive properties of cell lines were measured in a Matrigel-coated filter chamber assay. The values were 89.58%, 91.8%, and 39.5% for B16 LVc, B16, and B16 shR-SOCS-1, respectively, in three independent experiments.

Silencing of SOCS-1 Inhibits Tumor Cell Migration and Invasion

Cell migration was measured using a monolayer wound healing assay observed by phase-contrast microscopy with an inverted microscope. Images were taken at regular intervals during the course of 0 to 24 hours of both areas flanking the wound and the marker lines (=10 images). The cells silenced for SOCS-1 (B16 shR-SOCS-1) showed reduced migration, roughly one third of the control (Figure 2*A*). Furthermore, B16 shSOCS-1 significantly reduced the invasion when compared with the cell lines B16 LVc and B16 as demonstrated in Figure 2*B*.

SOCS-1 Acts as a Modulator of Resistance to Anoikis

As shown in Figure 3, the silencing of SOCS-1 abolished the capacity of melanoma cells to grow in soft agar, thus independently of substrate and cell-cell adhesion, which is a characteristic of metastatic tumor cells. SOCS-1 and the network of cell reactivity that includes this regulator then seem essential to determine resistance to anoikis.

Proliferation Rate of Tumor Cells Depends on SOCS-1 Expression

In growth curve assays, melanoma cells duplicated every 24 hours. Tumor cells with silenced SOCS-1 expression had a similar growth

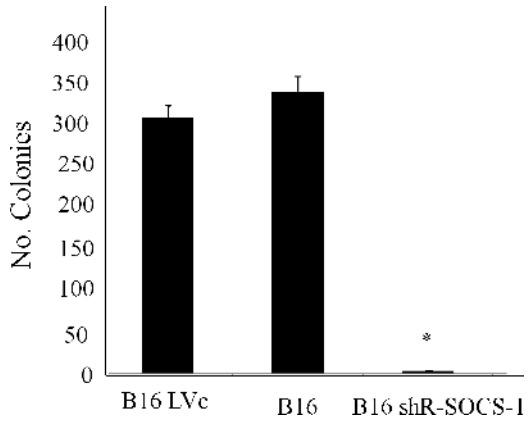

Figure 3. SOCS-1 protein is necessary for anoikis resistance: The silencing of SOCS-1 inhibits tumor cells resistance to anoikis as determined in a clonogenic assay. $^{**}P < .05$. Results average three independent experiments.

rate up to 72 hours, but this was delayed with time, being significantly reduced after 120 hours (Figure 4).

SOCS-1 Affects the Cell Cycle with Prolonged S Phase and Cell Division

Differences in the growth rate could reflect alterations in the cell cycle and in the expression of growth factor receptors. The cell cycles of the different cell lines were evaluated by FACS. As shown in Figure 5*A*, the silencing of SOCS-1 protein affected the cell cycle expanding the S phase. Prolonged DNA replication, hence of cell division, was reflected in the increased area of nuclei and cytoplasm (Figure 5, *B* and *C*). These results are coherent with the reduced growth rate in the shR-SOCS-1 cell line.

Silencing of SOCS-1 Protein Promotes Down-regulation of Growth Factor Receptors

Different receptor tyrosine kinases responding to insulin and growth factors were downregulated in melanoma cells after SOCS-1 silencing. This was assessed by determining the frequency of cells expressing tyrosine kinase receptors (TKRs) in the different cell lines including shR-SOCS-1. Specific antibodies were used for insulin receptor α and β chains, EGFR and phosphorylated EGFR, and three different FGFRs. As shown in Figure 6, shR-SOCS-1 showed, in comparison with the control cell lines, a significant down-regulation of TKRs particularly of p-EGFR, Ins-Rα, and FGFR-4 and -5. Signaling involving these TKRs modulates DNA synthesis, cell proliferation, migration, adhesion, metastasis, and survival.

Silencing SOCS-1 Inhibited Tumor Growth and Metastasis of Melanoma In Vivo

The tumorigenic and metastatic potentials of melanoma cells *in vivo* were virtually abolished by SOCS-1 silencing. All cell lines were injected subcutaneously into male C57Bl/6 mice, but although B16 and B16 LVc cells formed tumors of comparable size, the shR-SOCS-1 cell line was unable to grow *in vivo* (Figure 7*A*). Animal survival was also evaluated as shown in Figure 7*B*. With the control cell lines, all animals were dead or killed with tumors of maximum 3000 mm^3 before the 25th day of challenge. Two animals in the shR-SOCS-1 group died, but four were alive and tumor-less up to 70 days after challenge, when the experiment was terminated.

In the metastatic model, SOCS-1 protein silencing in melanoma cells gave rise to a limited number of lung metastases in mice (average of 75 nodules) when compared with B16 LVc and B16 cell lines (Figure 8*A*) that formed black masses of tumor growth in the lungs approximately three times that of tumor-less lungs (Figure 8, *B* and *C*).

Discussion

The evidence for the expression and functional activity of SOCS-1 in tumor cells is controversial. At the protein level, SOCS-1 is undetectable in normal human melanocytes and melanocytic nevi but uniformly expressed in melanoma cell lines [26]. Moreover, detection of SOCS-1 by immunohistochemistry was closely related to tumor invasiveness, thickness, and stage. Therefore, SOCS-1 was regarded as a progression marker of human melanoma and a component of tumor resistance against endogenous and/or administered cytokines. Aberrant expression of SOCS-1 in melanoma cells may promote cell proliferation and protect tumor cells against IFN-γ released in the microenvironment.

Compared with normal breast cells, a high constitutive expression of SOCS 2, 3, 5, 6, 7, CIS, and/or SOCS 1 genes was observed in human cancer cells [27]. In the MCF-7 and HCC1937 cell lines, the transcription of SOCS-1 was upregulated by IFN-α and/or ionizing radiation. In breast cancer cells, STAT3 pathway is constitutively activated, but the elevated expression of SOCS genes may confer resistance to proinflammatory cytokines by shutting down STAT1/STAT5 signaling.

Although SOCS-1 is also expressed in human prostate cancer both *in vitro* and *in vivo*, it exerts growth-inhibitory function by down-regulating cyclins D1 and E and cyclin-dependent kinases 2 and 4 [28]. In a brain metastatic melanoma cell line, the expression of SOCS-1 was reduced relative to that of the parental cell and the decreased SOCS-1 expression resulted in increased activation of

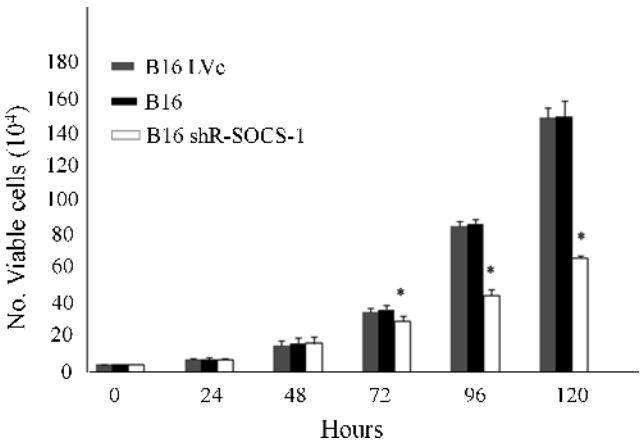

Figure 4. Melanoma cell growth kinetics depends on SOCS-1. *In vitro*, melanoma cells duplicate every 24 hours. Tumor cells with silenced SOCS-1 expression showed a similar growth rate up to 72 hours, but this was delayed with further incubation, being significantly reduced after 120 hours. $^{*}P < .05$. B16 LVc (gray bars), B16 (black bars), and B16 shR-SOCS-1 (white bars). Results average three independent experiments.

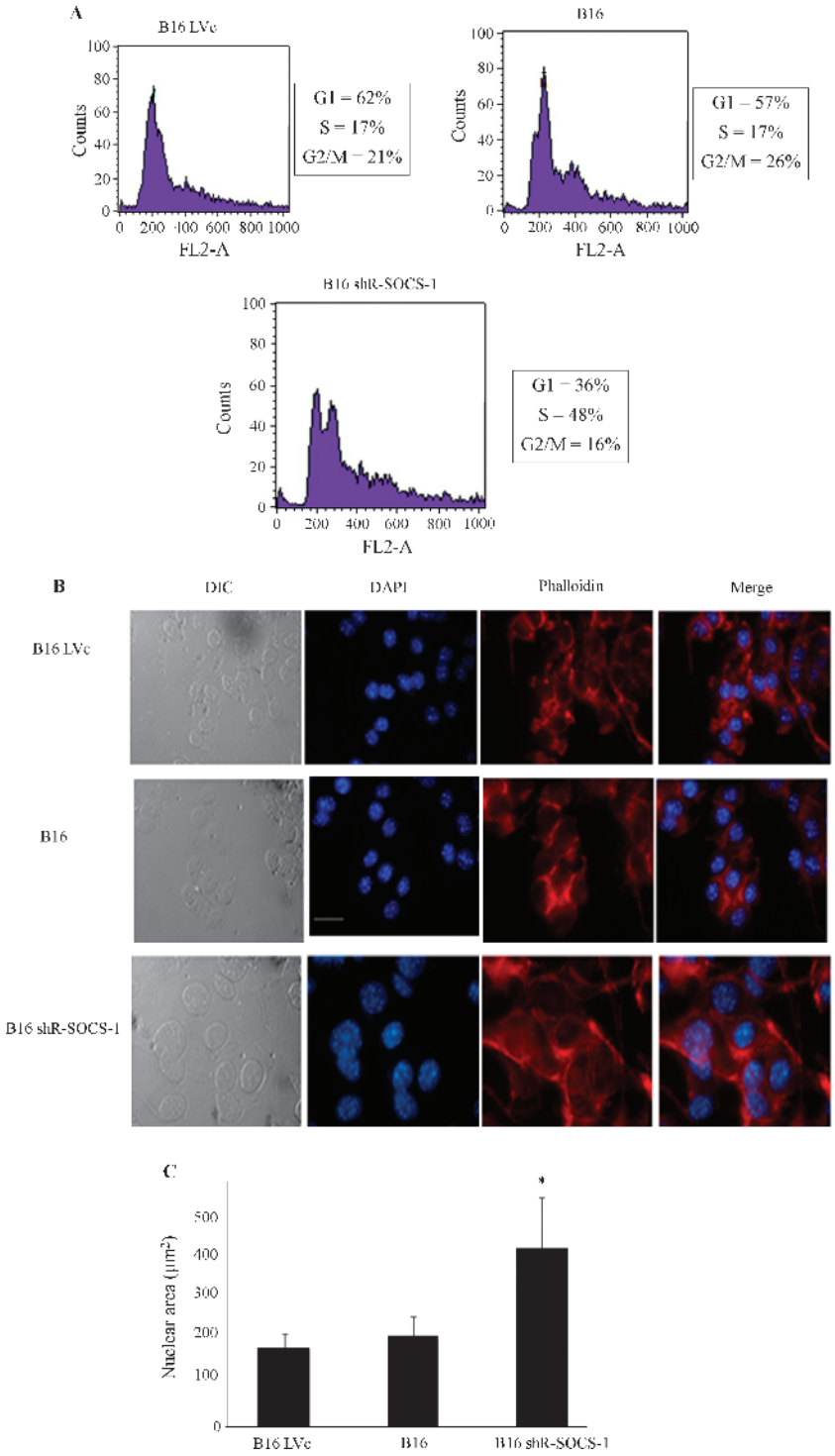

Figure 5. Silencing of SOCS-1 prolongs the S phase in the cell cycle. (A) Cell cycle phases of tumor cell lines are shown by FACScan flow cytometer with percent values. (B) Tumor cells (2×10^4) were seeded on sterilized round coverslips, permeabilized, and stained with phalloidin-TRITC (1:1000) and 1 mg/ml of DAPI diluted in PBS for 1 hour. The cells and nuclei of B16 shR-SOCS-1 cells have increased size compared with the control tumor cells. (C) Means of nuclear areas in the cell lines were calculated using two nuclear diameters ($A = \pi D/2d/2$).

STAT3 and overexpression of matrix metalloproteinase-2, basic fibroblast growth factor, and vascular endothelial growth factor, which promoted brain metastasis coherent with enhanced invasion and angiogenesis of melanoma cells [19]. These apparently contradictory effects suggest that SOCS-1 and other SOCS have different functions depending on the origin of the tumor.

In the present work, a stable system of SOCS-1 gene silencing using lentiviral particles was performed creating a variant of B16F10-Nex2 melanoma cell that was tested *in vitro* and *in vivo*. Generally, SOCS-1 silencing rendered cells with loss of function regarding cell proliferation, migration, invasion, tumor establishment *in vivo*, and tumor metastasis. In opposition to this response, methylation-dependent silencing of

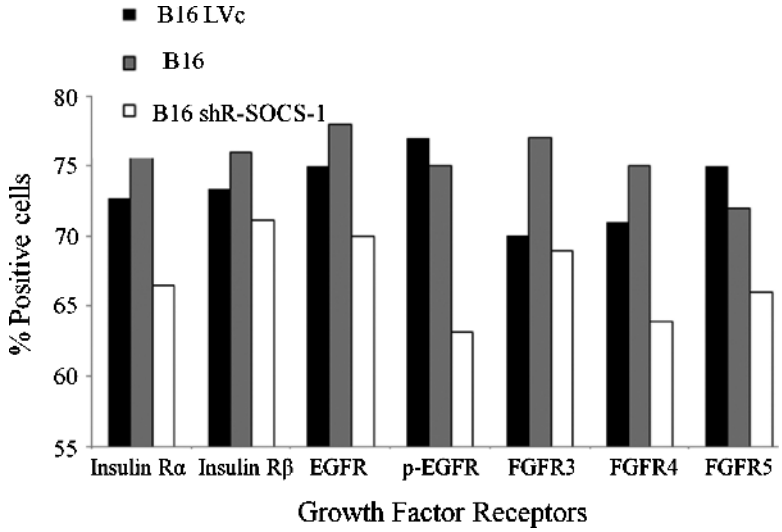

Figure 6. Melanoma growth factor receptors. Cell lines (10^6 cells in suspension) were fixed and analyzed by FACScan flow cytometry with antibodies specific for growth factor receptors. Data show the percent positive cells in 5×10^4 cells of B16 (black bars), B16 LVc (gray bars), and B16 shR-SOCS-1 (white bars) cell lines.

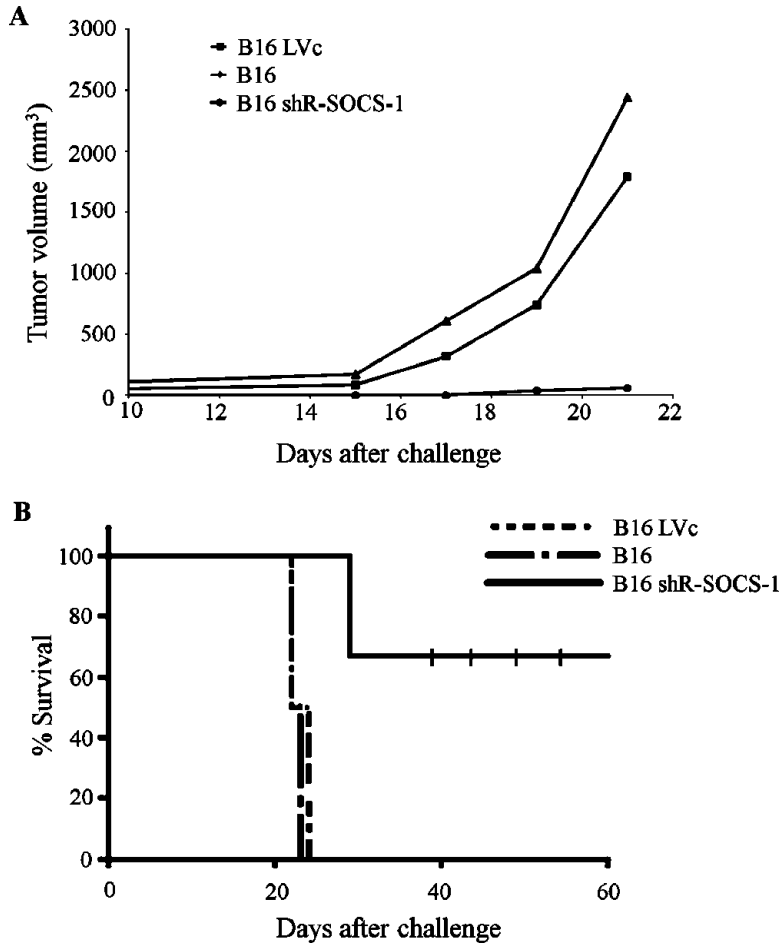

Figure 7. Silencing of SOCS-1 renders cells unable to grow *in vivo*. (A) In the subcutaneous model, tumors were produced by injecting 5×10^4 cells of each lineage into the right flanks of mice ($n = 6$, per cell line). The mean tumor volume of B16 shR-SOCS-1 was only 175 mm^3. (B) SOCS-1 silencing rendered cells of low aggressiveness with four of six tumor-free animals after 60 days of challenge.

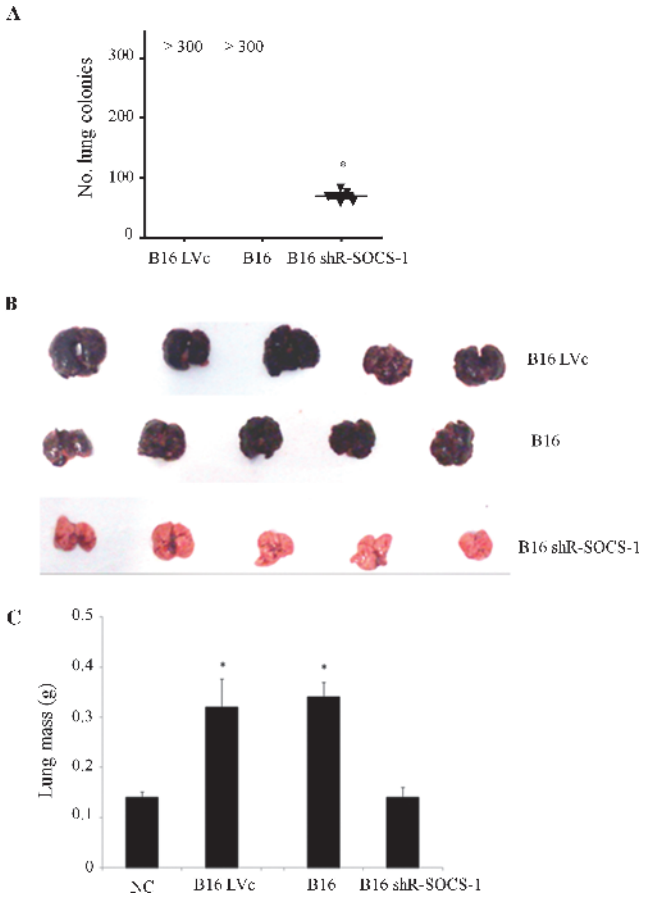

Figure 8. Tumor cells with silenced SOCS-1 are unable to metastasize. (A) In the metastatic model (lung colonization), 5×10^5 tumor cells of each cell line were injected into the tail veins of mice (0.1 ml per mouse). Fifteen days later, mice were killed, their lungs were harvested, and the number of macroscopic tumor nodules was counted ($n = 5$ per group). (B) Images of the lungs with high and low metastatic load. (C) Lung mass showing a nonsignificant increase with B16 shR-SOCS-1 cells compared with the B16 LVc and B16 control cell lines.

SOCS-3 and, to a lesser extent, the SOCS-1 gene in head and neck squamous cell and Barrett adenocarcinoma was associated with tumor growth *in vitro* and *in vivo* [30,31]. Also, the high frequency (65%) of aberrant SOCS-1 methylation in human hepatocellular carcinoma and the growth suppression caused by apoptosis on restoration in HCC cell lines of SOCS-1 points to the importance of the constitutive activation of the JAK/STAT pathway in tumor development [21].

In an attempt to understand the response of B16F10-Nex2 cells in the face of SOCS-1 silencing *in vitro* and *in vivo*, we focused on the growth control of melanoma cells. In comparison with normal melanocytes, melanoma cells are additionally stimulated by EGF/transforming growth factor α and nerve growth factor [32]. Other studies have shown that insulin and insulin growth factor stimulate melanoma cell growth, both *in vivo* and *in vitro* [33,34]. Insulin-resistant lines showed defective insulin receptor because of ATP-dependent partial proteolysis of the β subunit [35].

In the present work, we show that SOCS-1 silencing affected the expression of insulin receptor α-chain, EGFR (phosphorylated), and FGFR-4 and -5. There is evidence that SOCS-1 and SOCS-3 bind to EGFR and associate with insulin receptor substrates 1 and 2. In both cases, however, such interaction was regulatory. In the case of EGFR binding, SOCS proteins facilitated proteasomal degradation of the receptor [36]. As to the second interaction, SOCS-1 deficiency increased IRS-2 expression and enhanced hepatic insulin sensitivity *in vivo* [37]. In rat chondrosarcoma cells, however, binding of SOCS-1 to FGFR3 prolonged the half-life of the receptor, showing that it inhibited FGFR3 degradation possibly by recycling it to the plasma membrane [38]. Further, in this case, constitutive binding of SOCS-1 to FGFR3 changed the balance between STAT-1 and MAPK pathways, attenuating the former and enhancing the latter by extending the duration of the signal. It was suggested that SOCS-1 is not an exclusive signal inhibitor and may prolong MAPK signaling as described for SOCS-3 that binds to RasGAP [39]. A similar signaling could be operating in B16F10-Nex2 cells so that SOCS-1 silencing could be followed by increased degradation of insulin receptor, EGFR, and FGFR, leading to attenuation of the MAPK signaling that regulates downstream kinases or transcription factors, the phosphatidylinositol-3 kinase, and Akt antiapoptotic pathway. MAPK leads to the transcription of genes that are important for the cell cycle. Therefore, attenuation of MAPK signaling would be compatible with alterations in the cell cycle S phase, decreased proliferation, and decreased resistance to anoikis as observed in the present work.

The effects of SOCS-1 silencing *in vitro* clearly reflect on the loss of tumorigenesis *in vivo* as observed in B16F10-Nex2 cells, suggesting that this protein could be a target of chemotherapy depending on the cancer type and on the specific addressing of anti–SOCS-1 agents to the tumor cells.

References

[1] Gray-Schopfer V, Wellbrock C, and Marais R (2007). Melanoma biology and new targeted therapy. *Nature* **445**, 851–857.

[2] Grichnik JM (2008). Melanoma, nevogenesis, and stem cell biology. *J Invest Dermatol* **128**, 2365–2380.

[3] Dai CY, Haqq CM, and Puzas JE (2006). Molecular correlates of site-specific metastasis. *Semin Radiat Oncol* **16**, 102–110.

[4] Eccles SA (2005). Targeting key steps in metastatic tumour progression. *Curr Opin Genet Dev* **15**, 77–86.

[5] Lopez-Bergami P, Fitchman B, and Ronai Z (2008). Understanding signaling cascades in melanoma. *Photochem Photobiol* **84**, 289–306.

[6] Meier F, Schittek B, Busch S, Garbe C, Smalley K, Satyamoorthy K, Li G, and Herlyn M (2005). The RAS/RAF/MEK/ERK and PI3K/AKT signaling pathways present molecular targets for the effective treatment of advanced melanoma. *Front Biosci* **10**, 2986–3001.

[7] Jørgensen K, Holm R, Mælandsmo GM, and Flørenes VA (2003). Expression of activated extracellular signal–regulated kinases 1/2 in malignant melanomas: relationship with clinical outcome. *Clin Cancer Res* **9**, 5325–5331.

[8] Tsareva S, Moriggl R, Corvinus F, Wiederanders B, Schütz A, Kovacic B, and Friedrich K (2007). STAT3 activation promotes invasive growth of colon carcinomas through matrix metalloproteinase induction. *Neoplasia* **9**, 279–291.

[9] Kovacic B, Stoiber D, Moriggl R, Weisz E, Ott RG, Kreibich R, Levy DE, Beug H, Freissmuth M, and Sexl V (2006). STAT1 acts as a tumor promoter for leukemia development. *Cancer Cell* **10**, 77–87.

[10] Gamero AM, Young MR, Mentor-Marcel R, Bobe G, Scarzello AJ, Wise J, and Colburn NH (2010). STAT2 contributes to promotion of colorectal and skin carcinogenesis. *Cancer Prev Res (Phila)* **3**, 495–504.

[11] Ferrand A, Kowalski-Chauvel A, Bertrand C, Escrieut C, Mathieu A, Portolan G, Pradayrol L, Fourmy D, Dufresne M, and Seva C (2005). A novel mechanism for JAK2 activation by a G protein–coupled receptor, the CCK2R: implication of this signaling pathway in pancreatic tumor models. *J Biol Chem* **280**, 10710–10715.

[12] Senft C, Priester M, Polacin M, Schroder K, Seifert V, Kogel D, and Weissenberger J (2011). Inhibition of the JAK-2/STAT3 signaling pathway impedes the migratory and invasive potential of human glioblastoma cells. *J Neurooncol* **101**, 393–403.

[13] Starr R, Willson TA, Viney EM, Murray LJ, Rayner JR, Jenkins BJ, Gonda TJ, Alexander WS, Metcalf D, Nicola NA, et al. (1997). A family of cytokine-inducible inhibitors of signalling. *Nature* **387**, 917–921.

[14] Morita Y, Naka T, Kawazoe Y, Fujimoto M, Narazaki M, Nakagawa R, Fukuyama H, Nagata S, and Kishimoto T (2000). Signals transducers and activators of transcription (STAT)–induced STAT inhibitor-1 (SSI-1)/suppressor of cytokine signaling-1 (SOCS-1) suppresses tumor necrosis factor alpha–induced cell death in fibroblasts. *Proc Natl Acad Sci USA* **97**, 5405–5410.

[15] Song MM and Shuai K (1998). The suppressor of cytokine signaling (SOCS) 1 and SOCS3 but not SOCS2 proteins inhibit interferon-mediated antiviral and antiproliferative activities. *J Biol Chem* **273**, 35056–35062.

[16] Yoshimura A, Naka T, and Kubo M (2007). SOCS proteins, cytokine signalling and immune regulation. *Nat Rev Immunol* **7**, 454–465.

[17] Kamura T, Maenaka K, Kotoshiba S, Matsumoto M, Kohda D, Conaway RC, Conaway JW, and Nakayama KI (2004). VHL-box and SOCS-box domains determine binding specificity for Cul2-Rbx1 and Cul5-Rbx2 modules of ubiquitin ligases. *Genes Dev* **18**, 3055–3065.

[18] Vuong BQ, Arenzana TL, Showalter BM, Losman J, Chen XP, Mostecki J, Banks AS, Limnander A, Fernandez N, and Rothman PB (2004). SOCS-1 localizes to the microtubule organizing complex-associated 20S proteasome. *Mol Cell Biol* **24**, 9092–9101.

[19] Huang FJ, Steeg PS, Price JE, Chiu WT, Chou PC, Xie K, Sawaya R, and Huang S (2008). Molecular basis for the critical role of suppressor of cytokine signaling-1 in melanoma brain metastasis. *Cancer Res* **68**, 9634–9642.

[20] Yasukawa H, Misawa H, Sakamoto H, Masuhara M, Sasaki A, Wakioka T, Ohtsuka S, Imaizumi T, Matsuda T, Ihle JN, et al. (1999). The JAK-binding protein JAB inhibits Janus tyrosine kinase activity through binding in the activation loop. *EMBO J* **18**, 1309–1320.

[21] Yoshikawa H, Matsubara K, Qian GS, Jackson P, Groopman JD, Manning JE, Harris CC, and Herman JG (2001). SOCS-1, a negative regulator of the JAK/STAT pathway, is silenced by methylation in human hepatocellular carcinoma and shows growth-suppression activity. *Nat Genet* **28**, 29–35.

[22] Zitzmann K, Brand S, De Toni EN, Baehs S, Goke B, Meinecke J, Spottl G, Meyer HH, and Auernhammer CJ (2007). SOCS1 silencing enhances antitumor activity of type I IFNs by regulating apoptosis in neuroendocrine tumor cells. *Cancer Res* **67**, 5025–5032.

[23] Takahashi Y, Kaneda H, Takasuka N, Hattori K, Nishikawa M, Watanabe Y, and Takakura Y (2008). Enhancement of antiproliferative activity of interferons by RNA interference–mediated silencing of SOCS gene expression in tumor cells. *Cancer Sci* **99**, 1650–1655.

[24] Lesinski GB, Zimmerer JM, Kreiner M, Trefry J, Bill MA, Young GS, Becknell B, and Carson WE III (2010). Modulation of SOCS protein expression influences the interferon responsiveness of human melanoma cells. *BMC Cancer* **10**, 142.

[25] Fojtova M, Boudny V, Kovarik A, Lauerova L, Adamkova L, Souckova K, Jarkovsky J, and Kovarik J (2007). Development of IFN-γ resistance is associated with attenuation of SOCS genes induction and constitutive expression of SOCS 3 in melanoma cells. *Br J Cancer* **97**, 231–237.

[26] Li Z, Metze D, Nashan D, Muller-Tidow C, Serve HL, Poremba C, Luger TA, and Bohm M (2004). Expression of SOCS-1, suppressor of cytokine signalling-1, in human melanoma. *J Invest Dermatol* **123**, 737–745.

[27] Evans MK, Yu CR, Lohani A, Mahdi RM, Liu X, Trzeciak AR, and Egwuagu CE (2007). Expression of *SOCS1* and *SOCS3* genes is differentially regulated in breast cancer cells in response to proinflammatory cytokine and growth factor signals. *Oncogene* **26**, 1941–1948.

[28] Neuwirt H, Puhr M, Santer FR, Susani M, Doppler W, Marcias G, Rauch V, Brugger M, Hobisch A, Kenner L, et al. (2009). Suppressor of cytokine signaling (SOCS)-1 is expressed in human prostate cancer and exerts growth-inhibitory function through down-regulation of cyclins and cyclin-dependent kinases. *Am J Pathol* **174**, 1921–1930.

[29] Dobroff AS, Rodrigues EG, Moraes JZ, and Travassos LR (2002). Protective, anti-tumor monoclonal antibody recognizes a conformational epitope similar to melibiose at the surface of invasive murine melanoma cells. *Hybrid Hybridomics* **21**, 321–331.

[30] Weber A, Hengge UR, Bardenheuer W, Tischoff I, Sommerer F, Markwarth A, Dietz A, Wittekind C, and Tannapfel A (2005). SOCS-3 is frequently methylated in head and neck squamous cell carcinoma and its precursor lesions and causes growth inhibition. *Oncogene* **24**, 6699–6708.

[31] Tischoff I, Hengge UR, Vieth M, Ell C, Stolte M, Weber A, Schmidt WE, and Tannapfel A (2007). Methylation of SOCS-3 and SOCS-1 in the carcinogenesis of Barrett's adenocarcinoma. *Gut* **56**, 1047–1053.

[32] Krasagakis K, Garbe C, Zouboulis CC, and Orfanos CE (1995). Growth control of melanoma cells and melanocytes by cytokines. *Rec Res Cancer Res* **139**, 169–182.

[33] Sauter ER and Herlyn M (1998). Molecular biology of human melanoma development and progression. *Mol Carcinog* **23**, 132–143.

[34] Slominski A, Wortsman J, Carlson AJ, Matsuoka LY, Balch CM, and Mihm MC (2001). Malignant melanoma. *Arch Pathol Lab Med* **125**, 1295–1306.

[35] Slominski A, McNeely T, and Pawelek J (1992). Defect of insulin receptor in insulin-resistant variants of Cloudman S91 mouse melanoma cells. *Melanoma Res* **2**, 115–122.

[36] Xia L, Wang L, Chung AS, Ivanov SS, Ling MY, Dragoi AM, Platt A, Gilmer TM, Fu XY, and Chin YE (2002). Identification of both positive and negative domains within the epidermal growth factor receptor COOH-terminal region for signal transducer and activator of transcription (STAT) activation. *J Biol Chem* **277**, 30716–30723.

[37] Jamieson E, Chong MM, Steinberg GR, Jovanovska V, Fam BC, Bullen DV, Chen Y, Kemp BE, Proietto J, Kay TW, et al. (2005). Socs1 deficiency enhances hepatic insulin signaling. *J Biol Chem* **280**, 31516–31521.

[38] Ben Zvi T, Yayon A, Gertler A, and Monsonego-Ornan E (2006). Suppressors of cytokine signaling (SOCS) 1 and SOCS3 interact with and modulate fibroblast growth factor receptor signaling. *J Cell Sci* **119**, 380–387.

[39] Cacalano NA, Sanden D, and Johnston JA (2001). Tyrosine-phosphorylated SOCS-3 inhibits STAT activation but binds to p120 RasGAP and activates Ras. *Nat Cell Biol* **3**, 460–465.